SCIREA Journal of Mechanics

http://www.scirea.org/journal/Mechanics

December 29, 2016

Volume 1, Issue 2, December 2016

Structural-parametric models of electromagnetoelastic actuators for nano- and micromanipulators of mechatronic systems

Sergey M. Afonin

Department of Intellectual Technical Systems, National Research University of Electronic Technology (MIET), Moscow, Russia, 124498

Email: eduems@mail.ru

Abstract

Structural-parametric models, parametric structural schematic diagrams, transfer functions of electromagnetoelastic actuators for nano- and micromanipulators are obtained. Effects of geometric and physical parameters of electromagnetoelastic actuators and external load on its dynamic characteristics are determined. For calculations mechatronic systems with piezoactuators of nano- and micromanipulators the parametric structural schematic diagrams and the transfer functions of piezoactuators are obtained. A generalized parametric structural schematic diagram of the electromagnetoelastic actuator is constructed.

Keywords: Electromagnetoelastic actuator, deformation, nano- and micromanipulators, structural-parametric model, piezoactuator, parametric structural schematic diagram, transfer functions

1. Introduction and statement of problem

Electromechanical actuators for nano- and micromanipulators operate within working loads providing elastic deformations of actuators. Piezoactuator - piezomechanical device intended for actuation of mechanisms, systems or management based on the piezoelectric effect, converts electrical signals into mechanical movement or force. The application of electromechanical actuators based on electromagnetoelasticity (piezoelectric, piezomagnetic, electrostriction, and magnetostriction effects) is promising in nanotechnology, nanobiology, power engineering, microelectronics, astronomy for large compound telescopes, antennas satellite telescopes and adaptive optics equipment for precision matching, compensation of temperature and gravitation deformations, and atmospheric turbulence via wave front correction [1 − 4].

In the present paper is solving the problem of building the structural parametric model of the electromagnetoelastic actuator in contrast its electrical equivalent circuit [5 − 7]. By solving the wave equation with allowance methods of mathematical physics for the corresponding equation of electromagnetoelasticity, the boundary conditions on loaded working surfaces of a electromagnetoelastic actuator, and the strains along the coordinate axes, it is possible to construct a structural parametric model of the actuator. The transfer functions and the parametric structure schemes of the piezoactuators are obtained from a set of equations describing the corresponding structural parametric models of the piezoelectric actuators for nano- and micromanipulators of the mechatronic systems [8 − 21].

The piezoactuator of nanometric movements operates based on the inverse piezoeffect, in which the motion is achieved due to deformation of the piezoelement when an external electric voltage is applied to it. Piezoactuators for drives of nano- and micrometric movements provide a movement range from several nanometers to tens of microns, a sensitivity of up to 10 nm/V, a loading capacity of up to 1000 N, the power at the output shaft of up to 100 W, and a ransmission band of up to 1000 Hz [22].

The investigation of static and dynamic characteristics of a piezoactuator for nano- and micromanipulators as the control object is necessary for calculation the piezodrive for control systems of nano- and micrometric movements. At the nano- and microlevels, piezoactuators are used in linear nano- and microdrives and micropumps. Piezoactuators are used in the majority of nanomanipulators for scanning tunneling microscopes (STMs), scanning force microscopes (SFMs), and atomic force microscopes (AFMs). Nanorobotic manipulators with nano- and

microdisplacements with piezoactuators based are a key component in nano- and microdisplacement nanorobotic systems [23 − 28].

2.Structural-parametric models and transfer functions of electromagnetoelastic actuators

Deformation of the piezoactuator corresponds to its stressed state. If the mechanical stress T is created in the piezoelectric element, the deformation S is formed in it. There are six stress components T_1 , T_2 , T_3 , T_4 , T_5 , T_6 , the components T_1 - T_3 are related to extension-compression stresses, T_4 - T_6 to shear stresses.

The matrix state equations [7] connecting the electric and elastic variables for polarized ceramics have the form

$$\mathbf{D} = \mathbf{dT} + \boldsymbol{\varepsilon}^T \mathbf{E} , \tag{1}$$

$$\mathbf{S} = \mathbf{s}^E \mathbf{T} + \mathbf{d}^t \mathbf{E} . \tag{2}$$

Here, the first equation describes the direct piezoelectric effect, and the second - the inverse piezoelectric effect; $\mathbf{S}$ is the column matrix of relative deformations; $\mathbf{T}$ is the column matrix of mechanical stresses; $\mathbf{E}$ is the column matrix of electric field strength along the coordinate axes; $\mathbf{D}$ is the column matrix of electric induction along the coordinate axes; $\mathbf{s}^E$ is the elastic compliance matrix for $E = \text{const}$; and $\mathbf{d}^t$ is the the transposed matrix of the piezoelectric modules.

In polarized ceramics PZT there are five independent components s_{11}^E, s_{12}^E, s_{13}^E, s_{33}^E, s_{55}^E in the elastic compliance matrix, three independent components d_{33} , d_{31} , d_{15} in the transposed matrix of the piezoelectric modules and three independent components $\varepsilon_{11}^{\mathrm{T}}$, $\varepsilon_{22}^{\mathrm{T}}$, $\varepsilon_{33}^{\mathrm{T}}$ in the matrix of dielectric constants.

The equation of electromagnetoelasticity of the actuator [7] has the form

$$S_i = s_{ij}^{E,H,\Theta} T_j + d_{mi}^{H,\Theta} E_m + d_{mi}^{E,\Theta} H_m + \alpha_i^{E,H} \Delta\Theta , \tag{3}$$

where S_i is the relative deformation along the axis *i*, *E* is the electric field strength, *H* is the magnetic field strength, Θ is the temperature, $s_{ij}^{E,H,\Theta}$ is the elastic compliance for $E = \text{const}$, $H = \text{const}$, $\Theta = \text{const}$, T_j is the mechanical stress along the axis *j*, $d_{mi}^{H,\Theta}$ is the piezomodule, i.e.,

the partial derivative of the relative deformation with respect to the electric field strength for constant magnetic field strength and temperature, i.e., for $H = \text{const}$, $\Theta = \text{const}$, E_m is the electric field strength along the axis *m*, $d_{mi}^{E,\Theta}$ is the magnetostriction coefficient, H_m is the magnetic field strength along the axis *m*, $\alpha_i^{E,H}$ is the coefficient of thermal expansion, $\Delta\Theta$ is deviation of the temperature Θ from the value $\Theta = \text{const}$, $i = 1, 2, \ldots, 6$, $j = 1, 2, \ldots, 6$, $m = 1, 2, 3$.

When the electric and magnetic fields act on the electromagnetoelastic actuator separately, we have the equations [7]

as the equation of inverse piezoelectric effect:

$S_3 = d_{33}E_3 + s_{33}^E T_3$ for the longitudinal deformation when the electric field along axis 3 causes deformation along axis 3,

$S_1 = d_{31}E_3 + s_{11}^E T_1$ for the transverse deformation when the electric field along axis 3 causes deformation along axis 1,

$S_5 = d_{15}E_1 + s_{55}^E T_5$ for the shift deformation when the electric field along axis 1 causes deformation in the plane perpendicular to this axis,

as the equation of magnetostriction:

$S_3 = d_{33}H_3 + s_{33}^H T_3$ for the longitudinal deformation when the magnetic field along axis 3 causes deformation along axis 3,

$S_1 = d_{31}H_3 + s_{11}^H T_1$ for the transverse deformation when the magnetic field along axis 3 causes deformation along axis 1,

$S_5 = d_{15}H_1 + s_{55}^H T_5$ for the shift deformation when the magnetic field along axis 1 causes deformation in the plane perpendicular to this axis.

Let us consider the longitudinal piezoeffect in a piezoactuator shown in Figure 1, which represents a piezoplate of thickness δ with the electrodes deposited on its faces perpendicular to axis 3, the area of which is equal to S_0.

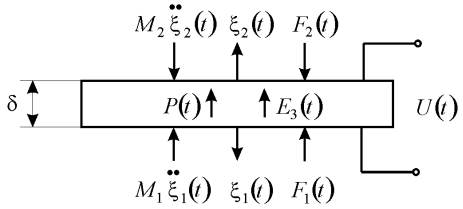

Figure 1. Piezoactuator for the longitudinal piezoeffect

The equation of the inverse the longitudinal piezoelectric effect [7, 9] has the following form:

$$S_3 = d_{33}E_3(t) + s_{33}^E T_3(x,t), \tag{4}$$

here, $S_3 = \partial\xi(x,t)/\partial x$ is the relative displacement of the cross section of the piezoactuator along axis 3, d_{33} is the piezoelectric modulus for the longitudinal piezoelectric effect, $E_3(t) = U(t)/\delta$ is the electric field strength, $U(t)$ is the voltage between the electrodes of actuator, δ is the thickness, s_{33}^E is the elastic compliance along axis 3, and T_3 is the mechanical stress along axis 3. The equation of equilibrium for the forces acting on the piezoactuator

$$T_3 S_0 = F + M\frac{\partial^2\xi(x,t)}{\partial t^2}, \tag{5}$$

where F is the external force applied to the piezoactuator, S_0 is the cross section area and M is the displaced mass.

For constructing a structural parametric model of the voltage-controlled piezoactuator, let us solve simultaneously the wave equation, the equation of the inverse longitudinal piezoelectric effect, and the equation of forces acting on the faces of the piezoactuator. Calculations of the piezoactuators are performed using a wave equation [2, 7] describing the wave propagation in a long line with damping but without distortions, which can be written as

$$\frac{1}{(c^E)^2}\frac{\partial^2\xi(x,t)}{\partial t^2} + \frac{2\alpha}{c^E}\frac{\partial\xi(x,t)}{\partial t} + \alpha^2\xi(x,t) = \frac{\partial^2\xi(x,t)}{\partial x^2}, \tag{6}$$

where $\xi(x,t)$ is the displacement of the section of the piezoelectric plate, x is the coordinate, t is time, c^E is the sound speed for $E = \text{const}$, α is the damping coefficient that takes into account the attenuation of oscillations caused by the energy dissipation due to thermal losses during the wave propagation. Using the Laplace transform, we can reduce the original problem for the partial differential hyperbolic equation of type (5) to a simpler problem for the linear ordinary differential equation [8, 9] with the parameter of the Laplace operator p.

Applying the Laplace transform to the wave equation (6)

$$\Xi(x,p) = L\{\xi(x,t\} = \int_0^\infty \xi(x,t)e^{-pt}dt\,, \tag{7}$$

and setting the zero initial conditions,

$$\xi(x,t)\big|_{t=0} = \frac{\partial\xi(x,t)}{\partial t}\bigg|_{t=0} = 0\,.$$

As a result, we obtain the linear ordinary second-order differential equation with the parameter p written as

$$\frac{d^2\Xi(x,p)}{dx^2} - \left[\frac{1}{(c^E)^2}p^2 + \frac{2\alpha}{c^E}p + \alpha^2\right]\Xi(x,p) = 0\,, \tag{8}$$

with its solution being the function

$$\Xi(x,p) = Ce^{-x\gamma} + Be^{x\gamma}\,, \tag{9}$$

where $\Xi(x,p)$ is the Laplace transform of the displacement of the section of the piezoelectric actuator, $\gamma = p/c^E + \alpha$ is the propagation coefficient. C and B are constant coefficients determining from the boundary conditions as

$$\Xi(0,p) = \Xi_1(p) \text{ for } x = 0 \tag{10}$$

$$\Xi(\delta,p) = \Xi_2(p) \text{ for } x = \delta$$

Then, the constant coefficients

$$C = \left(\Xi_1 e^{\delta\gamma} - \Xi_2\right)/\left[2\mathrm{sh}(\delta\gamma)\right], \quad B = \left(\Xi_1 e^{-\delta\gamma} - \Xi_2\right)/\left[2\mathrm{sh}(\delta\gamma)\right]. \tag{11}$$

Then, the solution (9) of the linear ordinary second-order differential equation can be written as

$$\Xi(x,p) = \left\{\Xi_1(p)\mathrm{sh}\left[(\delta - x)\gamma\right] + \Xi_2(p)\mathrm{sh}(x\gamma)\right\}/\mathrm{sh}(\delta\gamma)\,. \tag{12}$$

The equations for the forces operating on the faces of the piezoelectric actuator plate are as follows:

$$T_3(0,p)S_0 = F_1(p) + M_1p^2\Xi_1(p) \qquad \text{for} \quad x = 0\,, \tag{13}$$

$$T_3(\delta,p)S_0 = -F_2(p) + M_2p^2\Xi_1(p) \quad \text{for} \quad x = \delta\,,$$

where $T_3(0,p)$ and $T_3(\delta,p)$ are determined from the equation of the inverse piezoelectric effect.

For $x = 0$ and $x = \delta$, we obtain the following set of equations for determining stresses in the piezoactuator:

$$T_3(0,p)=\frac{1}{s_{33}^E}\left.\frac{d\Xi(x,p)}{dx}\right|_{x=0}-\frac{d_{33}}{s_{33}^E}E_3(p)\,, \tag{14}$$

$$T_3(\delta,p)=\frac{1}{s_{33}^E}\left.\frac{d\Xi(x,p)}{dx}\right|_{x=\delta}-\frac{d_{33}}{s_{33}^E}E_3(p)\,.$$

Equations (13) yield the following set of equations for the structural parametric model of the piezoactuator:

$$\Xi_1(p)=\left[1/\left(M_1p^2\right)\right]\left\{-F_1(p)+\left(1/\chi_{33}^E\right)\left[d_{33}E_3(p)-\left[\gamma/\mathrm{sh}(\delta\gamma)\right]\left[\mathrm{ch}(\delta\gamma)\Xi_1(p)-\Xi_2(p)\right]\right]\right\}, \tag{15}$$

$$\Xi_2(p)=\left[1/\left(M_2p^2\right)\right]\left\{-F_2(p)+\left(1/\chi_{33}^E\right)\left[d_{33}E_3(p)-\left[\gamma/\mathrm{sh}(\delta\gamma)\right]\left[\mathrm{ch}(\delta\gamma)\Xi_2(p)-\Xi_1(p)\right]\right]\right\},$$

where $\chi_{33}^E=s_{33}^E/S_0$. Figure 2 shows the parametric structure scheme of a voltage-controlled piezoactuator corresponding to (15) supplemented with an external circuit equation $U(p)=U_0(p)/(RC_0p+1)$, where $U_0(p)$ is the supply voltage, R is the resistance of the external circuit and C_0 is the static capacitance of the piezoactuator.

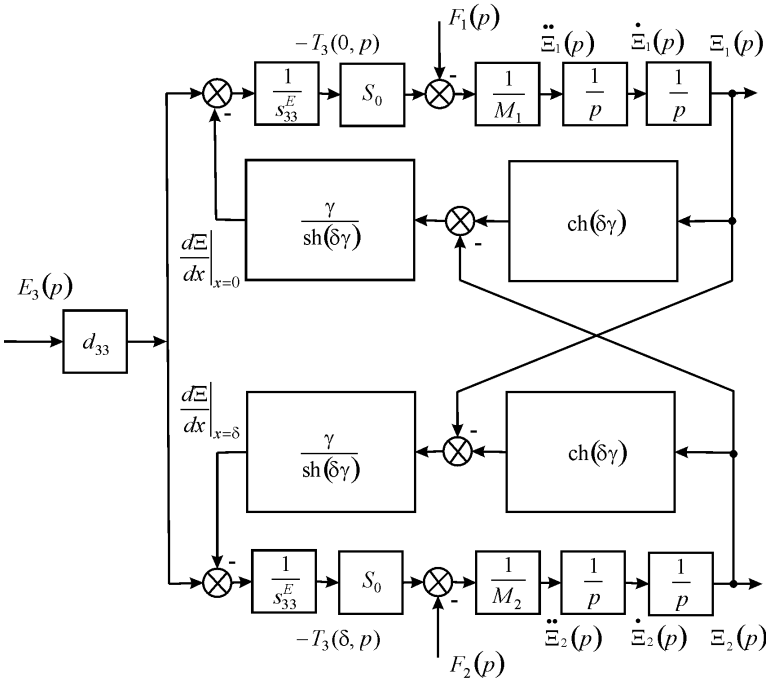

Figure 2. Parametric structural schematic diagram of a voltage-controlled piezoactuator for longitudinal piezoeffect

The equation of the inverse shift piezoelectric effect [7, 9] for piezoactuator Figure 3 has the following form:

$$S_5 = d_{15}E_1(t) + s_{55}^E T_5(x,t)\,, \tag{16}$$

here, $S_5 = \partial\xi(x,t)/\partial x$ is the relative displacement of the cross section of the piezoactuator along axis 5, d_{55} is the piezoelectric modulus for the shift piezoelectric effect, $E_1(t) = U(t)/\delta$ is the electric field strength along axis 1, $U(t)$ is the voltage between the electrodes of actuator, δ is the thickness, s_{55}^E is the elastic compliance along axis 5, and T_5 is the mechanical stress along axis 5.

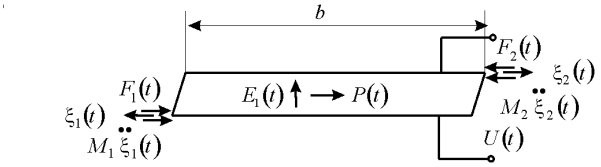

Figure 3. Piezoactuator for the shift piezoeffect

For piezoactuator of the shift piezoelectric effect Figure 3 we obtain the following set of equations describing the structural parametric model and parametric structural schematic diagram of piezoactuator Figure 4

$$\begin{aligned}&\Xi_1(p) = \left[1/\left(M_1 p^2\right)\right]\cdot\\ &\left\{-F_1(p) + \left(1/\chi_{55}^E\right)\left[d_{15}E_1(p) - \left[\gamma/\mathrm{sh}(b\gamma)\right]\left[\mathrm{ch}(b\gamma)\Xi_1(p) - \Xi_1(p)\right]\right]\right\},\end{aligned} \tag{17}$$

$$\begin{aligned}&\Xi_2(p) = \left[1/\left(M_2 p^2\right)\right]\cdot\\ &\left\{-F_2(p) + \left(1/\chi_{55}^E\right)\left[d_{15}E_1(p) - \left[\gamma/\mathrm{sh}(b\gamma)\right]\left[\mathrm{ch}(b\gamma)\Xi_2(p) - \Xi_1(p)\right]\right]\right\},\end{aligned}$$

where $\chi_{55}^E = s_{55}^E/S_0$.

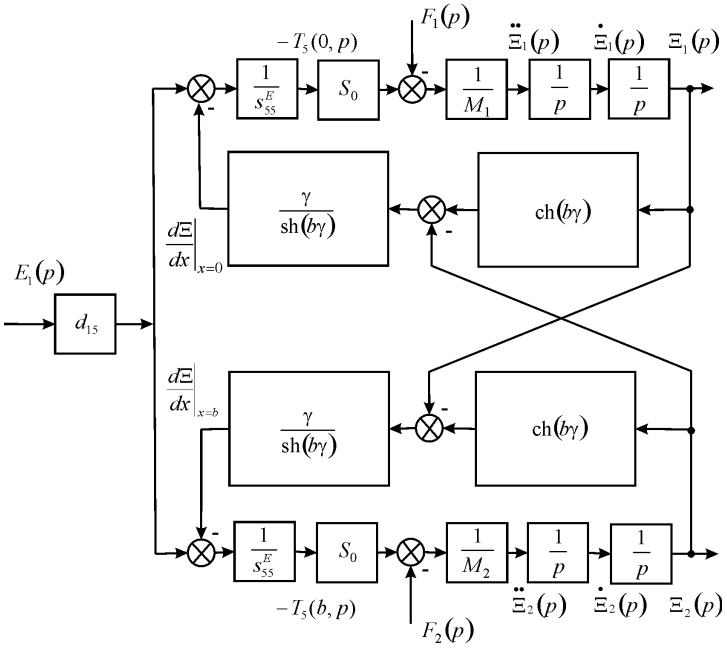

Figure 4. Parametric structural schematic diagram of a voltage-controlled piezoactuator for shift piezoeffect

Taking into account generalized electromagnetoelasticity equation (3), we obtain the following system of equations describing the generalized structural-parametric model of the electromagnetoelastic actuator for nano- and micromanipulators:

$$\Xi_1(p)=\left[1/\left(M_1p^2\right)\right]\left\{-F_1(p)+\left(1/\chi_{ij}^{\Psi}\right)\left[\nu_{mi}\Psi_m(p)-\left[\gamma/\mathrm{sh}(l\gamma)\right]\left[\mathrm{ch}(l\gamma)\Xi_1(p)-\Xi_2(p)\right]\right]\right\}, \tag{18}$$

$$\Xi_2(p)=\left[1/\left(M_2p^2\right)\right]\left\{-F_2(p)+\left(1/\chi_{ij}^{\Psi}\right)\left[\nu_{mi}\Psi_m(p)-\left[\gamma/\mathrm{sh}(l\gamma)\right]\left[\mathrm{ch}(l\gamma)\Xi_2(p)-\Xi_1(p)\right]\right]\right\},$$

where $\nu_{mi}=\begin{cases}d_{33},d_{31},d_{15}\\ g_{33},g_{31},g_{15}\\ d_{33},d_{31},d_{15}\end{cases}$, $\Psi_m=\begin{cases}E_3,E_1\\ D_3,D_1\\ H_3,H_1\end{cases}$, $s_{ij}^{\Psi}=\begin{cases}s_{33}^E,s_{11}^E,s_{55}^E\\ s_{33}^D,s_{11}^D,s_{55}^D\\ s_{33}^H,s_{11}^H,s_{55}^H\end{cases}$, $c^{\Psi}=\begin{cases}c^E\\ c^D\\ c^H\end{cases}$, $\gamma=\begin{cases}\gamma^E\\ \gamma^D\\ \gamma^H\end{cases}$, $l=\begin{cases}\delta\\ h\\ b\end{cases}$,

$\chi_{ij}^{\Psi}=s_{ij}^{\Psi}/S_0$, parameters Ψ of the control for the electromagnetoelastic actuator: *E* for voltage control, *D* for current control, *H* for magnetic field strength control. Figure 5 shows the generalized parametric block diagram of the electromagnetoelastic actuator corresponding to the set of equations (18).

Generalized structural-parametric model (18) of the electromagnetoelastic actuator after algebraic transformations provides the transfer functions of the electromagnetoelastic actuator for nano- and micromanipulators in the form of the ratio of the Laplace transform of the displacement of the transducer face and the Laplace transform of the corresponding force at zero initial conditions.

The joint solution of equations (18) for the Laplace transforms of displacements of two faces of the electromagnetoelastic actuator yields

$$\Xi_1(p) = W_{11}(p)\Psi_m(p) + W_{12}(p)F_1(p) + W_{13}(p)F_2(p), \tag{19}$$

$$\Xi_2(p) = W_{21}(p)\Psi_m(p) + W_{22}(p)F_1(p) + W_{23}(p)F_2(p).$$

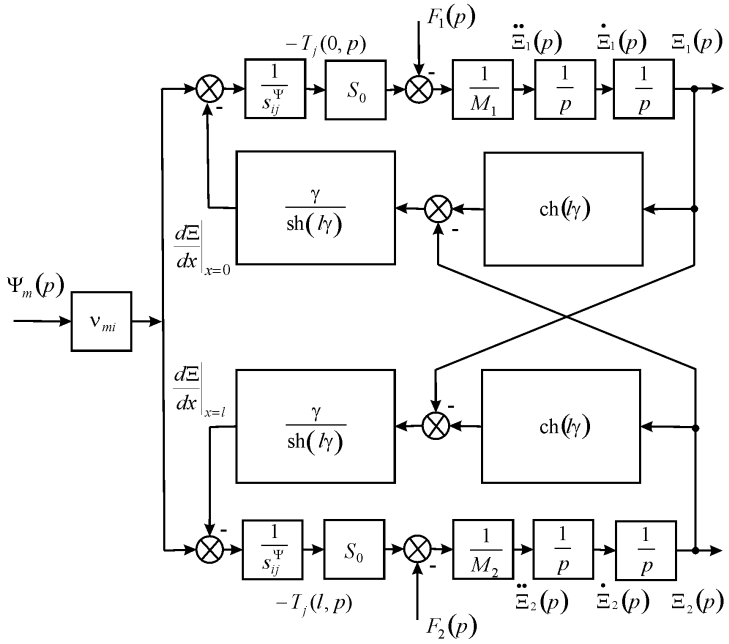

Figure 5. Generalized parametric structural schematic diagram of the electromagnetoelastic actuator

The generalized transfer functions of the electromagnetoelastic actuator are

$$W_{11}(p) = \Xi_1(p)/\Psi_m(p) = \nu_{mi}\left[M_2\chi_{ij}^{\Psi}p^2 + \gamma\mathrm{th}(l\gamma/2)\right]/A_{ij}, \quad \chi_{ij}^{\Psi} = s_{ij}^{\Psi}/S_0,$$

$$A_{ij} = M_1M_2\left(\chi_{ij}^{\Psi}\right)^2 p^4 + \left\{(M_1+M_2)\chi_{ij}^{\Psi}/\left[c^{\Psi}\mathrm{th}(l\gamma)\right]\right\}p^3 + \left[(M_1+M_2)\chi_{ij}^{\Psi}\alpha/\mathrm{th}(l\gamma) + 1/\left(c^{\Psi}\right)^2\right]p^2 + 2\alpha p/c^{\Psi} + \alpha^2,$$

$$W_{21}(p) = \Xi_2(p)/\Psi_m(p) = \nu_{mi}\left[M_1\chi_{ij}^{\Psi}p^2 + \gamma\mathrm{th}(l\gamma/2)\right]/A_{ij},$$

$$W_{12}(p) = \Xi_1(p)/F_1(p) = -\chi_{ij}^{\Psi}\left[M_2\chi_{ij}^{\Psi}p^2 + \gamma/\mathrm{th}(l\gamma)\right]/A_{ij},$$

$$W_{13}(p) = \Xi_1(p)/F_2(p) = W_{22}(p) = \Xi_2(p)/F_1(p) = \left[\chi_{ij}^{\Psi}\gamma/\mathrm{sh}(l\gamma)\right]/A_{ij},$$

$$W_{23}(p) = \Xi_2(p)/F_2(p) = -\chi_{ij}^{\Psi}\left[M_1\chi_{ij}^{\Psi}p^2 + \gamma/\mathrm{th}(l\gamma)\right]/A_{ij}.$$

We obtain from equations (19) the generalized matrix equaion for the electromagnetoelastic actuator in the matrix form for nano- and micromanipulators

$$\begin{pmatrix} \Xi_1(p) \\ \Xi_2(p) \end{pmatrix} = \begin{pmatrix} W_{11}(p) & W_{12}(p) & W_{13}(p) \\ W_{21}(p) & W_{22}(p) & W_{23}(p) \end{pmatrix} \begin{pmatrix} \Psi_m(p) \\ F_1(p) \\ F_2(p) \end{pmatrix}. \quad (20)$$

Let us find the displacement of the faces the electromagnetoelastic actuator in a stationary regime for $\Psi_m(t) = \Psi_{m0} \cdot 1(t)$, $F_1(t) = F_2(t) = 0$ and inertial load. The static displacement [24 − 26] of the faces the electromagnetoelastic actuator $\xi_1(\infty)$ and $\xi_2(\infty)$ can be written in the following form:

$$\xi_1(\infty) = \lim_{t\to\infty} \xi_1(t) = \lim_{\substack{p\to 0 \\ \alpha\to 0}} pW_{11}(p)\Psi_{m0}/p = \nu_{mi} l \Psi_{m0} (M_2 + m/2)/(M_1 + M_2 + m), \quad (21)$$

$$\xi_2(\infty) = \lim_{t\to\infty} \xi_2(t) = \lim_{\substack{p\to 0 \\ \alpha\to 0}} pW_{21}(p)\Psi_{m0}/p = \nu_{mi} l \Psi_{m0} (M_1 + m/2)/(M_1 + M_2 + m), \quad (22)$$

$$\xi_1(\infty) + \xi_2(\infty) = \lim_{t\to\infty} (\xi_1(t) + \xi_2(t)) = \nu_{mi} l \Psi_{m0}, \quad (23)$$

where m is the mass of the electromagnetoelastic actuator, M_1, M_2 are the load masses.

Let us consider a numerical example of the calculation of static characteristics of the piezoactuator from piezoceramics PZT under the longitudinal piezoelectric effect at $m \ll M_1$ and $m \ll M_2$. For $d_{33} = 4 \cdot 10^{-10}$ m/V, $U = 250$ V, $M_1 = 10$ kg and $M_2 = 40$ kg we obtain the static displacement of the faces of the piezoactuator $\xi_1(\infty) = 80$ nm, $\xi_2(\infty) = 20$ nm, $\xi_1(\infty) + \xi_2(\infty) = 100$ nm.

The static displacement the faces of the piezoactuator for the transverse piezoelectric effect and inertial load at $U(t) = U_0 \cdot 1(t)$, $E_3(t) = E_{30} \cdot 1(t) = (U_0/\delta) \cdot 1(t)$ and $F_1(t) = F_2(t) = 0$ can be written in the following form:

$$\xi_1(\infty) = \lim_{t\to\infty} \xi_1(t) = \lim_{\substack{p\to 0 \\ \alpha\to 0}} pW_{11}(p)(U_0/\delta)/p = d_{31}(h/\delta) U_0 (M_2 + m/2)/(M_1 + M_2 + m), \quad (24)$$

$$\xi_2(\infty) = \lim_{t\to\infty} \xi_2(t) = \lim_{\substack{p\to 0 \\ \alpha\to 0}} pW_{21}(p)(U_0/\delta)/p = d_{31}(h/\delta) U_0 (M_1 + m/2)/(M_1 + M_2 + m), \quad (25)$$

$$\xi_1(\infty) + \xi_2(\infty) = \lim_{t\to\infty} (\xi_1(t) + \xi_2(t)) = d_{31}(h/\delta) U_0. \quad (26)$$

The static displacement of the faces of the piezoactuator for the transverse piezoelectric effect and inertial load at $m \ll M_1$ and $m \ll M_2$

$$\xi_1(\infty) = \lim_{t\to\infty} \xi_1(t) = \lim_{\substack{p\to 0 \\ \alpha\to 0}} pW_{11}(p)(U_0/\delta)/p = d_{31}(h/\delta) U_0 M_2/(M_1 + M_2), \quad (27)$$

$$\xi_2(\infty)=\lim_{t\to\infty}\xi_2(t)=\lim_{\substack{p\to 0\\ \alpha\to 0}} pW_{21}(p)(U_0/\delta)/p=d_{31}(h/\delta)U_0 M_1/(M_1+M_2). \tag{28}$$

Let us consider a numerical example of the calculation of static characteristics of the piezoactuator from piezoceramics PZT under the transverse piezoelectric effect at $m \ll M_1$ and $m \ll M_2$. For $d_{31}=2.5\cdot 10^{-10}$ m/V, $h=4\cdot 10^{-2}$ m, $\delta=2\cdot 10^{-3}$ m, $U=400$ V, $M_1=10$ kg and $M_2=40$ kg we obtain the static displacement of the faces of the piezoelectric actuator $\xi_1(\infty)=1600$ nm, $\xi_2(\infty)=400$ nm, $\xi_1(\infty)+\xi_2(\infty)=2$ μm.

Let us consider the description of the piezoactuator for the longitudinal piezoelectric effect for one rigidly fixed face of the transducer at $M_1 \to \infty$, therefore, we obtain from equation (20) the transfer functions of the piezoactuator for the longitudinal piezoelectric effect [12 − 17] in the following form:

$$W_{21}(p)=\Xi_2(p)/E_3(p)=d_{33}\delta/\left[M_2\delta\chi_{33}^E p^2+\delta\gamma\,\mathrm{cth}(\delta\gamma)\right], \tag{29}$$

If $M_1 \to \infty$ and $M_2=0$, an expression for the transfer function of unloaded piezoactuator under the longitudinal piezoelectric effect has the form

$$W_{21}(p)=\Xi_2(p)/E_3(p)=d_{33}/[\gamma\,\mathrm{cth}(\delta\gamma)]. \tag{30}$$

Now, using equation (30), we write the expression for the transfer function of unloaded piezoactuator under the transverse piezoelectric effect at $M_1 \to \infty$ and $M_2=0$

$$W_{21}(p)=\Xi_2(p)/E_3(p)=d_{31}/[\gamma\,\mathrm{cth}(h\gamma)]. \tag{31}$$

We write the resonance condition $\mathrm{ctg}(\omega h/c^E)=0$.

This means that the piezoactuator is a quarter-wave vibrator with the resonance frequency $f_r=c^E/(4h)$.

The transfer function of an unloaded piezoactuator under the transversal piezoeffect with voltage control, when $M_1 \to \infty$ and $M_2=0$, has the form

$$W_2(p)=\Xi_2(p)/U(p)=\Xi_2(p)/[E_3(p)\delta]=(d_{31}h/\delta)/\left[h\gamma\,\mathrm{cth}(h\gamma)\right]. \tag{32}$$

Accordingly, its frequency transfer function is described by the relation

$$W_2(j\omega)=\Xi_2(j\omega)/U(j\omega)=(d_{31}h/\delta)\mathrm{th}\left[h(j\omega/c^E+\alpha)\right]/\left[h(j\omega/c^E+\alpha)\right]. \tag{33}$$

Let us consider the static responses of the piezoactuator under the longitudinal piezoeffects. Let us determine the value of the The static displacement of the face of the piezoactuator $\xi_2(\infty)$ in

the static regime for $U(t)=U_0\cdot 1(t)$ and $F_2(t)=0$ or $F_2(t)=F_0\cdot 1(t)$ and $U(t)=0$.

Accordingly, the static displacement $\xi_2(\infty)$ of the piezoactuator under the longitudinal piezoeffect in the form

$$\xi_2(\infty)=\lim_{t\to\infty}\xi_2(t)=\lim_{\substack{p\to 0\\ \alpha\to 0}} pW_2(p)U_0/p=\lim_{\substack{p\to 0\\ \alpha\to 0}} d_{33}U_0\,\mathrm{th}(\alpha\delta)/(\alpha\delta)=d_{33}U_0, \tag{34}$$

$$\xi_2(\infty)=\lim_{\substack{p\to 0\\ \alpha\to 0}} pW_{23}(p)F_0/p=-\lim_{\substack{p\to 0\\ \alpha\to 0}}\left[\delta^2 F_0\,\mathrm{th}(\alpha\delta)\right]/\left[m(c^E)^2\alpha\delta\right]=-\delta s_{33}^E F_0/S_0. \tag{35}$$

Let us consider a numerical example of the calculation of static characteristics of the piezoactuator under the longitudinal piezoeffects. For $d_{33}=4\cdot 10^{-10}$ m/V, $U=300$ V, we obtain $\xi_2(\infty)=120$ nm. For $\delta=6\cdot 10^{-4}$ m, $s_{33}^E=3.5\cdot 10^{-11}$ m^2/N, $F_0=1000$ N, $S_0=1.75\cdot 10^{-4}$ m^2, we obtain $\xi_2(\infty)=-120$ nm. The experimental and calculated values for the piezoactuator are in agreement to an accuracy of 5%.

Let us consider the operation at low frequencies for the piezoactuator with one face rigidly fixed so that $M_1\to\infty$ and $m\ll M_2$. Representing $W_{21}(p)$ and $W_{23}(p)$ as

$$W_{21}(p)=\Xi_2(p)/E_3(p)=d_{33}\delta/\left[M_2\delta\chi_{33}^E p^2+\delta\gamma\,\mathrm{cth}(\delta\gamma)\right], \tag{36}$$

$$W_{23}(p)=\Xi_2(p)/F_2(p)=-\delta\chi_{33}^E/\left[M_2\delta\chi_{33}^E p^2+\delta\gamma\,\mathrm{cth}(\delta\gamma)\right]. \tag{37}$$

Using the approximation of the hyperbolic cotangent by two terms of the power series in transfer functions (36) and (37), at $m\ll M_2$ we obtain the following expressions the transfer functions in the frequency range of $0<\omega<0{,}01c^E/\delta$

$$W_{21}(p)=\Xi_2(p)/E_3(p)=d_{33}\delta/\left(T_t^2p^2+2T_t\xi_t p+1\right), \tag{38}$$

$$W_{23}(p)=\Xi_2(p)/F_2(p)=-\left(s_{33}^E\delta/S_0\right)/\left(T_t^2p^2+2T_t\xi_t p+1\right), \tag{39}$$

$$T_t=\left(\delta/c^E\right)\sqrt{M_2/m}=\sqrt{M_2/C_{33}^E},\quad \xi_t=(\alpha\delta/3)\sqrt{m/M_2},\quad C_{33}^E=S_0/\left(s_{33}^E\delta\right)=1/\left(\chi_{33}^E\delta\right).$$

where T_t is the time constant and ξ_t is the damping coefficient, C_{33}^E - is the is rigidity of the piezoactuator under the longitudinal piezoeffect.

In the static mode of operation the piezoactuator for mechatronic systems and elastic load we obtain the equation the following form

$$\frac{\xi_2}{\xi_{2m}}=\frac{1}{1+C_e/C_{33}^E}, \tag{40}$$

where ξ_2 is the displacement of the piezoactuator in the case of the elastic load, $\xi_{2m} = d_{33}U_0$ is the maximum displacement of the piezoactuator, C_e is the load rigidity.

Equations (38, 40) yield the transfer function of the piezoelectric actuator with a fixed end and elastic inertial load in the following form

$$W_2(p) = \frac{\Xi_2(p)}{U(p)} = \frac{d_{33}}{\left(1 + C_e / C_{33}^E\right)\left(T_t^2 p^2 + 2T_t \xi_t p + 1\right)}, \tag{41}$$

where the time constant T_t and the damping coefficient ξ_t are determined by the formulas

$$T_t = \sqrt{M_2 / \left(C_e + C_{33}^E\right)}, \ \xi_t = \alpha\delta^2 C_{33}^E \Big/ \left(3c^E \sqrt{M\left(C_e + C_{33}^E\right)}\right).$$

Let us consider the operation at low frequencies for the piezoelectric actuator with one face rigidly fixed so that $M_1 \to \infty$ and $m << M_2$ for $M_2 = 40$ kg, $C_{33} = 9 \cdot 10^6$ N/m, $C_e = 10^6$ N/m we obtain $T_t = 2 \cdot 10^{-3}$ c.

3. Results and Discussions

Taking into account equation of generalized electromagnetoelasticity (piezoelectric, piezomagnetic, electrostriction, and magnetostriction effects) and decision wave equation we obtain a generalized parametric structural schematic diagram of electromagnetoelastic actuator Figure 5 for nano- and micromanipulators. The results of constructing a generalized structural-parametric model and parametric structural schematic diagram of electromagnetoelastic actuator [2-4] for the longitudinal, transverse and shift deformations are shown in Figure 5. Parametric structural schematic diagrams piezoactuators for longitudinal piezoeffect Figure 2, for transverse piezoeffect and for shift piezoeffect Figure 4 converts to generalized parametric structural schematic diagram of the electromagnetoelastic actuator Figure 5 with the replacement of the parameters

$$\Psi_m = E_3, E_3, E_1; \ \nu_{mi} = d_{33}, d_{31}, d_{15}; \ s_{ij}^{\Psi} = s_{33}^E, s_{11}^E, s_{55}^E; \ l = \delta, h, b.$$

Generalized structural-parametric model and generalized parametric structural schematic diagram of the electromagnetoelastic actuator after algebraic transformations provides the transfer functions of the electromagnetoelastic actuator for nano- and micromanipulators [9-26]. The piezoactuator with the transverse piezoelectric effect compared to the piezoactuator for the longitudinal piezoelectric effect provides a greater range of static displacement and less working

force. The magnetostriction actuators provides a greater range of static working forces [24-26].

Using the solutions of the wave equation of the electromagnetoelastic actuator and taking into account the features of the deformations along the coordinate axes, it is possible to construct the generalized structural-parametric model, generalized parametric structural schematic diagram and the transfer functions of the electromagnetoelastic actuator for nano- and micromanipulators.

4. Conclusions

Thus, using the obtained solutions of the wave equation and taking into account the features of the deformations along the coordinate axes, it is possible to construct the generalized structural-parametric model and parametric structural schematic diagram of the electromagnetoelastic actuator for nano- and micromanipulators and to describe its dynamic and static properties with allowance for the physical properties, the external load during its operation as a part of the the mechatronic system.

The transfer functions and the parametric structural schematic diagrams of the piezoactuators for the transverse, longitudinal and shift piezoelectric effects are obtained from structural parametric models of the piezoactuators for nano- and micromanipulators of the mechatronic systems.

References:

[1] Uchino, K. (1997) Piezoelectric actuator and ultrasonic motors. Boston, MA: Kluwer Academic Publisher, 347 p.

[2] Afonin, S.M. (2006) Solution of the wave equation for the control of an elecromagnetoelastic transduser. *Doklady mathematics*, 73, 2, 307-313, doi:10.1134/S1064562406020402.

[3] Afonin, S.M. (2008) Structural parametric model of a piezoelectric nanodisplacement transduser. *Doklady physics*, 53, 3, 137-143, doi:10.1134/S1028335808030063.

[4] Afonin, S.M. (2014) Stability of strain control systems of nano-and microdisplacement piezotransducers. *Mechanics of solids*, 49, 2, 196-207, doi:10.3103/S0025654414020095.

[5] Yang, Y. , Tang, L. (2009) Equivalent circuit modeling of piezoelectric energy harvesters, *Journal of intelligent material systems and structures*, 20, 18, 2223-2235.

[6] Cady, W.G. (1946) Piezoelectricity an introduction to the theory and applications of electromechancial phenomena in crystals. New York, London: McGraw-Hill Book Company, 806 p.

[7] Physical Acoustics: Principles and Methods. (1964) Vol.1. Part A. Methods and Devices. Ed.: W. Mason. New York: Academic Press. 515 p.

[8] Zwillinger, D. (1989) Handbook of Differential Equations. Boston: Academic Press. 673 p.

[9] Afonin, S.M. (2015) Structural-parametric model and transfer functions of electroelastic actuator for nano- and microdisplacement, Chapter 9 in *Piezoelectrics and Nanomaterials: Fundamentals, Developments and Applications*. Ed. I.A. Parinov. New York: Nova Science. pp. 225-242.

[10] Afonin, S.M. (2005) Generalized parametric structural model of a compound elecromagnetoelastic transduser. *Doklady physics*, 50, 2, 77-82, doi:10.1134/1.1881716.

[11] Afonin, S.M. (2015) Optimal control of a multilayer submicromanipulator with a longitudinal piezo effect. *Russian engineering research*, 35, 12, 907-910, doi:10.3103/S1068798X15120035.

[12] Afonin, S.M. (2002) Parametric structural diagram of a piezoelectric converter. *Mechanics of solids*, 37, 6, 85-91.

[13] Afonin, S.M. (2003) Deformation, fracture, and mechanical characteristics of a compound piezoelectric transducer. *Mechanics of solids*, 38, 6, 78-82.

[14] Afonin, S.M. (2004) Parametric block diagram and transfer functions of a composite piezoelectric transducer. *Mechanics of solids*, 39, 4, 119-127.

[15] Afonin, S.M. (2007) Elastic compliances and mechanical and adjusting characteristics of composite piezoelectric transducers. *Mechanics of solids*, 42, 1, 43-49, doi:10.3103/S0025654407010062.

[16] Afonin, S.M. (2009) Static and dynamic characteristics of a multy-layer electroelastic solid. *Mechanics of solids*, 44, 6, 935-950, doi:10.3103/S0025654409060119.

[17] Afonin, S.M. (2010) Design static and dynamic characteristics of a piezoelectric nanomicrotransducers. *Mechanics of solids*, 45, 1, 123-132, doi:10.3103/S0025654410010152.

[18] Afonin, S.M. (2001) Structural-parametric model of nanometer-resolution piezomotor. *Russian engineering research*, 21, 5, 42-50.

[19] Afonin, S.M. (2002) Parametric structure of composite nanometric piezomotor. *Russian engineering research*, 22, 12, 9-24.

[20] Afonin, S.M. (2011) Electromechanical deformation and transformation of the energy of a nano-scale piezomotor. *Russian engineering research*, 31, 7, 638-642, doi:10.3103/S1068798X11070033.

[21] Afonin, S.M. (2011) Electroelasticity problems for multilayer nano- and micromotors. *Russian engineering research*, 31, 9, 842-847, doi:10.3103/S1068798X11090036.

[22] Afonin, S.M. (2012) Nano- and micro-scale piezomotors. *Russian engineering research*, 32, 7-8, 519-522, doi:10.3103/S1068798X12060032.

[23] Afonin, S.M. (2015) Dynamic characteristics of multilayer piezoelectric nano- and micromotors. *Russian engineering research*, 35, 2, 89-93, doi:10.3103/S1068798X15020045.

[24] Afonin, S.M. (2005) Generalized structural parametric model of an elecromagnetoelastic transduser for control system of nano- and microdisplacement: I. Solution of the wave equation for control problem of an elecromagnetoelastic transduser. *Journal of computer and systems sciences international*, 44, 3, 399-405.

[25] Afonin, S.M. (2005) Generalized structural parametric model of an elecromagnetoelastic transduser for control system of nano- and microdisplacements: II. On the generalized structural parametric model of a compound elecromagnetoelastic transduser. *Journal of computer and systems sciences international*, 44, 4, 606-612.

[26] Afonin, S.M. (2006) Generalized structural-parametric model of an elecromagnetoelastic converter for nano- and micrometric movement control systems: III. Transformation parametric structural circuits of an elecromagnetoelastic converter for nano- and micromovement control systems. *Journal of computer and systems sciences international*, 45, 2, 317-325, doi:10.1134/S106423070602016X.

[27] Afonin, S.M. (2015) Block diagrams of a multilayer piezoelectric motor for nano- and microdisplacements based on the transverse piezoeffect. *Journal of computer and systems sciences international*, 54, 3, 424-439, doi:10.1134/S1064230715020021.

[28] Afonin, S.M. (2006) Absolute stability conditions for a system controlling the deformation of an elecromagnetoelastic transduser. *Doklady mathematics*, 74, 3, 943-948, doi:10.1134/S1064562406060391.